



Ab initio full charge-density study of the atomic volume of γ -phase Fr, Ra, Ac, Th, Pa, U, Np, and Pu

Vitos, Levente; Kollár, J.; Skriver, Hans Lomholt

Published in:
Physical Review B

Link to article, DOI:
[10.1103/PhysRevB.55.4947](https://doi.org/10.1103/PhysRevB.55.4947)

Publication date:
1997

Document Version
Publisher's PDF, also known as Version of record

[Link back to DTU Orbit](#)

Citation (APA):
Vitos, L., Kollár, J., & Skriver, H. L. (1997). Ab initio full charge-density study of the atomic volume of γ -phase Fr, Ra, Ac, Th, Pa, U, Np, and Pu. *Physical Review B*, 55(8), 4947-4952. <https://doi.org/10.1103/PhysRevB.55.4947>

General rights

Copyright and moral rights for the publications made accessible in the public portal are retained by the authors and/or other copyright owners and it is a condition of accessing publications that users recognise and abide by the legal requirements associated with these rights.

- Users may download and print one copy of any publication from the public portal for the purpose of private study or research.
- You may not further distribute the material or use it for any profit-making activity or commercial gain
- You may freely distribute the URL identifying the publication in the public portal

If you believe that this document breaches copyright please contact us providing details, and we will remove access to the work immediately and investigate your claim.

***Ab initio* full charge-density study of the atomic volume of α -phase Fr, Ra, Ac, Th, Pa, U, Np, and Pu**

L. Vitos and J. Kollár

Research Institute for Solid State Physics, P. O. Box 49, H-1525 Budapest, Hungary

H. L. Skriver

Center for Atomic-scale Materials Physics and Physics Department, Technical University of Denmark, DK-2800 Lyngby, Denmark

(Received 2 November 1995)

We have used a full charge-density technique based on the linear muffin-tin orbitals method in first-principles calculations of the atomic volumes of the light actinides including Fr, Ra, and Ac in their low-temperature crystallographic phases. The good agreement between the theoretical and experimental values along the series support the picture of itinerant $5f$ electronic states in Th to Pu. The increased deviation between theory and experiment found in Np and Pu may be an indication of correlation effects not included in the local density approximation. [S0163-1829(97)06408-4]

I. INTRODUCTION

To date, it is generally accepted that the light actinide metals form a transition series with a substantial f bonding. Part of the support for such an itinerant picture of the $5f$ electrons is supplied by the fact that modern one-electron theory yields atomic volumes for these elements which agree quite well with the experimental values.^{1,2} Furthermore, since f bonding is expected to give rise to complex crystal structures the appearance of tetragonal, orthorhombic, and monoclinic structures in the actinide series lends additional support to the itinerant $5f$ picture. In fact, even the fcc structure of Th is caused by the $5f$ electrons,³ and therefore all the light actinides from Th to Pu are considered to form a $5f$ transition series.

In spite of their success, the validity of the original linear muffin-tin orbitals (LMTO) calculations¹ may be questioned because the authors used the atomic sphere approximation (ASA), neglected spin-orbit interaction, and treated only the close-packed fcc phase. It is therefore not surprising that the equilibrium volumes of the light actinides have been recalculated several times, gradually reducing the number of approximations involved.⁴⁻⁹ However, although the calculational schemes have progressed considerably it is only recently that one has been able to calculate the atomic volumes of U, Np, and Pu in their α phases.¹⁰

To calculate the equilibrium volumes of the α phases of the actinide metals with up to 16 atoms per primitive cell one needs not only efficient computer codes but also to go beyond the ASA. One approach is to use a full-potential LMTO method as is done by Wills and co-workers.^{6,8,9} Another is to retain some of the efficiency of the ASA by using a spherically symmetric potential to calculate the kinetic energy and to generate the nonspherically symmetric charge density that is subsequently used in the evaluation of the remainder of the energy functional. In the present work we have adopted the latter full charge-density (FCD) approach, which was originally implemented in order to treat lattice distortions as well as open crystal structures such as those found in the actinide

series. The FCD method has been applied successfully in the calculation of the surface energies of the $4d$ metals¹¹ and the light actinides,¹² as well as the atomic volumes and elastic constants of the $4d$ metals.¹³

The calculated atomic volumes of the light actinides found in the literature show considerable scatter. For instance, the local-density atomic radius for fcc Th varies from 3.79 bohr in the original LMTO-ASA calculation¹ to 3.52 bohr in the recent full-potential calculation.⁹ The question is therefore whether one can trust the ASA result, which deviates by only 1% from the experimental value of 3.76 bohr,¹⁴ or whether the presumably more accurate full-potential result, which deviates by as much as 6%, means that the local-density approximation is inadequate for the light actinides. The full-potential calculations⁹ also include results obtained by the generalized gradient correction to the local-density approximation and this improves the agreement with experiment for Th to 3%. However, in view of the success of the full-potential calculations for the $4d$ series¹⁵ where the gradient correction approximation for Zr, which has approximately the same number of d electron as Th, leads to complete agreement with experiment, deviations of 6% and 3% for Th indicate either inadequate numerical approximations or a failure of the local density and the generalized gradient correction approximations.

In this situation it is important to evaluate the atomic radii of the light actinides by means of a one-electron method that is different from the previously applied methods and thereby obtain a second opinion, as it were. The FCD method is one such method that has been thoroughly tested, e.g., in calculations of the atomic radii of the $4d$ metals. It is found that the local-density FCD radii¹³ of the $4d$ metals from Y to Pd on the average are 1% larger than the corresponding local-density full-potential values¹⁵ and the deviation is traced to the fact that the kinetic energy in the FCD approach is calculated within the ASA. Since the remainder of the energy functional is evaluated correctly, also in crystal structures that are not close packed, we expect the FCD approach to yield atomic radii that are within 1% of the true local-density radii for the light actinides.

II. FULL CHARGE-DENSITY METHOD

In the full charge-density method¹¹ the kinetic energy of the local-density functional is calculated completely within the ASA, except for the inclusion of the so-called combined correction,^{16,17} by means of a spherically symmetrized charge density, while the Coulomb and the exchange and correlation contributions are calculated by means of the complete, nonspherically symmetric charge density within non-overlapping, space-filling Wigner-Seitz cells. In the first application^{11,12} the charge density was expressed in terms of an LMTO-ASA one-center expansion corrected in the outer corners of the Wigner-Seitz (WS) cell by a simple polynomial to maintain normalization over the cell. Here, we improve the accuracy of the one-center expansion by the use of the tail-cancellation theorem to correct the charge density in the overlap regions. In the following we give a brief outline of the method with special emphasis on the construction of the charge density.

A. Energy functional

The FCD energy functional is based on a spherically symmetric atomic-sphere potential. Within the local-density approximation we define

$$E_{FCD}[n(\mathbf{r})] = \sum_{\mathbf{R}} T_{ASA}^R + E[n(\mathbf{r})], \quad (1)$$

where

$$T_{ASA}^R = \int^{E_F} \epsilon N^R(\epsilon) d\epsilon - \frac{1}{\sqrt{4\pi}} \int_{S_R} n_0^{R,ASA}(r) V_{eff}^R(r) d^3r \quad (2)$$

is the kinetic energy per site evaluated in the ASA and

$$E[n(\mathbf{r})] = \int v_{ext}(\mathbf{r}) n(\mathbf{r}) d\mathbf{r} + \frac{1}{2} \int \int \frac{n(\mathbf{r}) n(\mathbf{r}')}{|\mathbf{r} - \mathbf{r}'|} d\mathbf{r} d\mathbf{r}' + \int \epsilon_{xc}[n(\mathbf{r})] n(\mathbf{r}) d\mathbf{r}. \quad (3)$$

In these equations E_F is the Fermi level, $N^R(\epsilon)$ the site-projected one-electron-state density, S_R the atomic Wigner-Seitz radius, $n_0^{R,ASA}(r)$ the $l=0$ component of the electronic charge density at the site \mathbf{R} , $V_{eff}^R(r)$ the effective one-electron potential corresponding to the ASA energy functional, $v_{ext}(\mathbf{r})$ the potential from the nuclei, $n(\mathbf{r})$ the total electronic charge density that is constructed from the output of a self-consistent ASA calculation and reflects the proper symmetry of the lattice, and ϵ_{xc} stands for the exchange-correlation energy density.

B. Charge density

It was shown by Andersen *et al.*^{18,19} that even for open structures such as the diamond structure one may obtain good charge densities by means of an LMTO-ASA potential. In their approach, however, the output charge density is given in a multicenter form which requires double lattice summations and is therefore less suitable in total energy calculations. Our aim is to rewrite the output ASA charge density in a one-center form

$$n^R(\mathbf{r}_R) = \sum_L n_L^R(r_R) Y_L(\hat{\mathbf{r}}_R), \quad (4)$$

where L is shorthand notation for (l, m) , Y_L is a real harmonic, and \mathbf{r}_R is measured from the origin of the cell at \mathbf{R} , i.e., $\mathbf{r}_R = \mathbf{r} - \mathbf{R}$. This expression is simple to evaluate and well suited for the integration in the Wigner-Seitz cell at \mathbf{R} .

The muffin-tin (MT) orbitals may be defined¹⁹ as

$$\chi_{RL}(E, \kappa, \mathbf{r}_R) = Y_L(\hat{\mathbf{r}}_R) \begin{cases} \varphi_{Rl}(E, r_R) + P_{Rl}(E, \kappa) j_l(\kappa, r_R) & \text{for } r_R \leq S_R \\ n_l(\kappa, r_R) & \text{for } r_R > S_R, \end{cases} \quad (5)$$

where $\varphi_{Rl}(E, r_R)$ is solution of the radial Schrödinger equation, $\kappa^2 \equiv E - V_0$ is the “kinetic energy in the interstitial region,” j_l and n_l are, respectively, regular and irregular solutions at the origin of the radial wave equation for the constant potential V_0 (the muffin-tin zero), and $P_{Rl}(E, \kappa)$ is the potential function. If the secular equation is satisfied and the MT spheres do not overlap, the wave function is given within one MT sphere either by the multicenter

$$\psi(E, \mathbf{r}) = \sum_{RL} \chi_{RL}(E, \kappa, \mathbf{r}_R) u_{RL} \quad (6)$$

or by the one-center form

$$\psi(E, \mathbf{r}_{R'}) = \sum_{L'} \varphi_{R'L'}(E, \kappa, \mathbf{r}_{R'}) u_{R'L'} \quad \text{if } r_{R'} \leq S_{R'}. \quad (7)$$

In the case of overlapping spheres, there is, in the region of overlap, an uncanceled remainder which is the superposition of the functions

$$f_{RL}(E, \kappa, \mathbf{r}_R) \equiv \chi_{RL}(E, \kappa, \mathbf{r}_R) - n_L(\kappa, \mathbf{r}_R) = f_{Rl}(E, \kappa, r_R) Y_L(\hat{\mathbf{r}}_R) \Theta_R(\mathbf{r}_R) \quad (8)$$

coming from the neighboring sites.¹⁹ Here,

$$f_{Rl}(E, \kappa, r_R) = \varphi_{Rl}(E, r_R) + P_{Rl}(E, \kappa) j_l(\kappa, r_R) - n_l(\kappa, r_R), \quad (9)$$

and $\Theta_R(\mathbf{r}_R)$ is a step function, which is 1 inside and zero outside the MT sphere at \mathbf{R} . Thus, in the case of overlapping spheres centered at \mathbf{R} the wave function at $\mathbf{R}'=0$ can be written as¹⁹

$$\psi(E, \mathbf{r}) = \sum_{L'} \varphi_{0L'}(E, \kappa, \mathbf{r}) u_{0L'} + \sum_R \sum_{L'} f_{RL'}(E, \kappa, \mathbf{r}_R) u_{RL'} \quad \text{if } r \leq S_0. \quad (10)$$

Here and in the following we use the notation \mathbf{r} for \mathbf{r}_0 .

In the conventional LMTO-ASA method with energy-independent MTOs and with $\kappa^2=0$ the function $f_{Rl}(r_R)$ has the form

$$f_{Rl}(r_R) = \left[\varphi_{Rl}(E_{vRl}, r_R) - \dot{\varphi}_{Rl}(E_{vRl}, r_R)(E_{vRl} - C_{Rl}) - \left(\frac{r_R}{S} \right)^{-l-1} \sqrt{2\Delta_{Rl}/S} \left[1 + \frac{E_{vRl} - C_{Rl}}{\Delta_{Rl}} \gamma_{Rl} \right] \right], \quad (11)$$

where $\dot{\varphi}_{Rl}(E_{vRl}, r_R)$ is the orthogonal energy derivative of the normalized function $\varphi_{Rl}(E_{vRl}, r_R)$, E_{vRl} , C_{Rl} , γ_{Rl} , and Δ_{Rl} are the usual LMTO potential parameters, while S is the average Wigner-Seitz radius.

If the radial function $f_{Rl}(r_R)$ may be approximated by a linear combination of Bessel functions

$$f_{Rl}(r_R) = \sum_i C_{Rl}^i K_l(k_i r_R), \quad (12)$$

(we use the spherical Hankel functions of first kind with $k_i^2 < 0^{20}$), we may use the expansion theorem to express the functions centered at the neighboring sites \mathbf{R} with the coordinates measured from the origin

$$f_{Rl}(r_R) Y_L(\hat{\mathbf{r}}_R) = \sum_{L'} f_{RLL'}(r) Y_{L'}(\hat{\mathbf{r}}). \quad (13)$$

For the $\Theta_R(\mathbf{r}_R)$ function this expansion may be carried out analytically, it is shown in the Appendix. After summing up the square of the wave functions for the occupied states and after some manipulation we obtain the following expression for the partial component of the charge density in Eq. (4):

$$n_L^0(r) = \sum_{R'L'R''L''}^{pq} G_{R'L'R''L''}^{pqL}(r) m_{R'L'R''L''}^{pq}. \quad (14)$$

Here, the function $G_{R'L'R''L''}^{pqL}(r)$ may be expressed in terms of $\varphi_{Rl}(E_{vRl}, r)$, $\dot{\varphi}_{Rl}(E_{vRl}, r)$, $f_{RLL'}(r)$, and the expansion coefficients of the function $\Theta_R(\mathbf{r}_R)$. These expressions and the definition of the energy moments, $m_{R'L'R''L''}^{pq}$ are given in the Appendix. A few examples of the application of the above formula for calculating charge density contours are given in Ref. 21.

C. Coulomb energy

To calculate the Coulomb energy in Eq. (3) we divide the solid into nonoverlapping, space filling cells around each lattice site. The total electrostatic energy of the system may be divided into contributions E^R belonging to the cell at \mathbf{R} , which are compounded of *intracell* and *intercell* terms. For simplicity, we only give expressions for the contribution corresponding to the cell centered at the origin, i.e.,

$$E^0 = E_{intra}^0[n^0] + E_{inter}^0[\{Q_L^R\}], \quad (15)$$

where we indicate that the intercell energy contribution depends on the multipole moments defined as

$$Q_L^R = \frac{(4\pi)^{1/2}}{2l+1} \int_{W-S \text{ cell at } \mathbf{R}} \left(\frac{r_R}{S} \right)^l n^R(\mathbf{r}_R) Y_L(\hat{\mathbf{r}}_R) d\mathbf{r}_R. \quad (16)$$

The intracell energy may be determined in the usual way, e.g., by numerical solution of the l -dependent Poisson equation

inside the bounding spheres, while the intercell interaction energy belonging to the cell at the origin may be written in the following form:^{22,23}

$$\begin{aligned} E_{inter}^0[\{Q_L^R\}] = & -\frac{1}{2S} \sum_L \sum_{\mathbf{R}} \frac{1}{2l+1} \left(\frac{b_R}{S} \right)^l Y_L(\hat{\mathbf{b}}_R) \\ & \times \sum_{L', L''} Q_{L'}^0 \frac{4\pi(2l''-1)!!}{(2l-1)!!(2l'-1)!!} \\ & \times C_{L', L''}^L \delta_{l'', l+1'} \sum_{L'''} S_{L'', L'''}(\mathbf{R} + \mathbf{b}_R) Q_{L'''}^R, \end{aligned} \quad (17)$$

where $S_{L, L'}(\mathbf{R})$ are the conventional LMTO structure constants and $C_{L', L''}^L$ a real-harmonic Gaunt coefficient. In Eq. (17) \mathbf{R} runs over the lattice vectors. For neighboring cells with overlapping bounding spheres (with the radii S_C^0 and S_C^R) the vector \mathbf{b}_R must be larger than zero to ensure the l convergence of the summations. An optimal choice for b_R is

$$b_R + R = \left(1 + \frac{1}{2\alpha} \right) (S_C^0 + S_C^R). \quad (18)$$

A reasonable choice for the parameter α is described in Ref. 23.

D. Computational details

In the calculations we used the scalar-relativistic, second-order LMTO Hamiltonian within the frozen-core approximation and included the combined correction.¹⁶⁻¹⁸ The valence electrons were treated self-consistently within the local-density approximation (LDA) with the Perdew-Zunger parametrization²⁴ of the results of Ceperley and Alder.²⁵ We included the $6p$ semicore states (first panel) together with the $5f$, $6d$, and $7s$ states (second panel) as band states. In the first panel we down-folded^{26,27} the s , d , and f states and in the second only the p states. This procedure accounts correctly for the important weak hybridization in the occupied parts of the bandstructure and reduces the rank of the eigenvalue problem to that of the number of active orbitals, i.e., three for the lower panel and 13 for the upper panel. The k -point sampling was performed on a uniform grid in the irreducible wedge of the Brillouin zones of the α structures using 225, 675, 392, 75, and 48 k points for Th, Pa, U, Np, and Pu, respectively.

III. ATOMIC VOLUME OF THE ACTINIDES

The results of the full charge-density calculations for the early actinides including Fr, Ra, and Ac in their low-temperature crystallographic α phases are presented in Fig. 1 and Table I. It is seen that the agreement between the calculated equilibrium atomic Wigner-Seitz radii and those obtained experimentally¹⁴ is quite satisfactory over the whole series. Because the calculations treat the $5f$ electrons as itinerant and not as localized, corelike states, in which case one finds extremely high volumes,⁵ one may conclude that the $5f$ electrons in the early actinides, i.e., before Am, are bonding electrons and that local-density theory gives a good de-

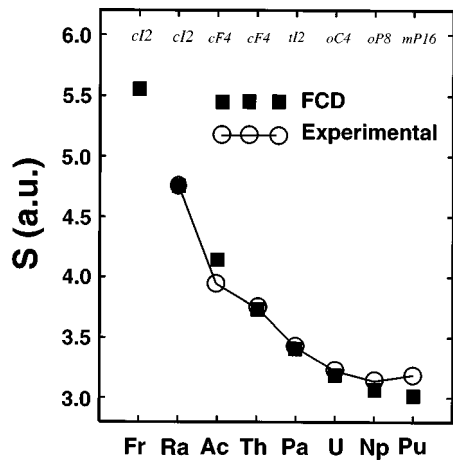


FIG. 1. Full charge-density (FCD) results for the equilibrium Wigner-Seitz radii of the first eight elements in the seventh row of the periodic table compared with experimental values¹⁴. The calculations have been performed in the LDA for the crystallographic α phases indicated in Pearson notation at the top of the figure.

scription of the ground state of these metals.

In the comparison between theory and experiments one finds a systematic overestimate of the binding, i.e., lowering of the calculated volume relative to the experimental volume, as one approaches Pu. One also observes that this trend is unaffected by the appearance of the distorted α phases in Pa—Pu. The deviation is therefore most easily interpreted as due to correlation effects not included in the presently used local-density approximation. However, before one reaches such a conclusion one must ascertain that the deviation may

not be caused by approximations, numerical or otherwise, in the technique used to solve the effective one-electron (Kohn-Sham) equations, i.e., that the calculated atomic volumes represent a close approximation to the true local-density values.

The only major approximation that remains in our implementation of the full charge-density method is the neglect of spin-orbit coupling. The effect of this approximation has been addressed in LMTO-ASA calculations,^{4,5} Table I, and in full-potential calculations.⁶ Brooks⁴ found an increase in atomic volume between Np and Pu and concluded that part of the deviation in Pu could be accounted for by spin-orbit coupling. A similar conclusion may be reached from the calculations by Söderlind *et al.*⁵ In contrast, the work of Wills and Eriksson,⁶ based on fully relativistic calculations, concluded that spin-orbit coupling did not lead to an increase in atomic volume between Np and Pu and therefore could not account for the deviation between theory and experiments in these metals.

Recently, Wills and co-workers^{6,8,9} have calculated the atomic volumes of Th, Pa, U, and Np in their α phases by means of the full-potential LMTO method. As may be seen in Fig. 2 and Table I, where we compare the full potential and full charge-density results, the agreement with the present atomic volumes is not good. In fact, because the full-potential method involves fewer approximations than the present full charge-density technique, it would appear that the 6% difference in calculated atomic radius (18% in volume) for Th disqualifies the present values for the whole series as the true local-density results. Obviously the close agreement between theory and experiment obtained in the

TABLE I. Atomic Wigner-Seitz radii in bohr for the light actinides in their low-temperature crystallographic phases, upper panel, and in the fcc structure, lower panel. The calculated values were all obtained within the local-density approximation. In the upper panel we list full charge-density and full-potential results and in the lower panel ASA results.

	Fr	Ra	Ac	Th	Pa	U	Np	Pu
Structure	cI2	cI2	cF4	cF4	tI2	oC4	oP8	mP16
Expt. ^a		4.790	3.922	3.756	3.422	3.221	3.142	3.182
Present	5.570	4.778	4.130	3.748	3.407	3.198	3.066	3.018
Wills ^b				3.558	3.281	3.097		
Eriksson ^c				3.64	3.38	3.12	2.99	
Söderlind ^d				3.517	3.280	3.092	2.991	
Structure	cF4	cF4	cF4	cF4	cF4	cF4	cF4	cF4
Skriver ^e	5.425	4.730	4.165	3.785	3.445	3.255	3.030	2.980
Söderlind ^f				3.814	3.496	3.256	3.107	3.015
Brooks ^g			4.188	3.773	3.396	3.227	3.097	3.091
Söderlind ^h				3.799	3.487	3.276	3.129	3.151

^aReference 14.

^bTable I, Ref. 6.

^cFigure 1, Ref. 8 and Fig. 11, Ref. 6.

^dLocal-density results, Ref. 9.

^ePure ASA results, Ref. 1.

^fASA plus combined correction, Ref. 5.

^gASA plus spin orbit, Ref. 4.

^hASA plus combined correction and spin orbit, Ref. 5.

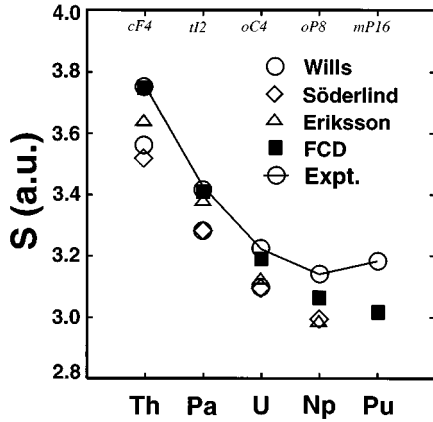


FIG. 2. Comparison between calculated Wigner-Seitz radii for the light actinides in their crystallographic α phases. Open circles from Ref. 6, open diamonds from Ref. 9, open triangles from Ref. 8, and filled squares from the present FCD calculations. Open circles with solid line are experimental values from Ref. 14.

present work is not a measure of the accuracy of the physical and numerical approximations of the FCD approach, but if numerical accuracy can be established it is a measure of the validity of the local-density approximation.

The four sets of LMTO-ASA calculations presented in Table I assumed the fcc structure,¹ included spin-orbit coupling,⁴ combined-correction,⁵ or combined-correction and spin-orbit coupling.⁵ These calculations all made use of the pressure relation²⁸ rather than the total energy to obtain equilibrium radii, and this procedure is relatively insensitive to the presence of the $6p$ semicore states to be discussed below. The atomic radii obtained in these calculations agree with each other to within less than 1%, which may be considered satisfactory. The only exception is Pu, where spin-orbit coupling leads to an increase in atomic radius of 5%. Thus, if one neglects Pu, it seems that small deviations in numerical techniques results in a scatter of approximately 1% in the calculated atomic radii. Hence, we may consider this number as an *ad hoc* measure of confidence.

Since we cannot assess the accuracy of the numerical implementation of the full-potential method^{6,8,9} we must judge the accuracy of the FCD calculations on the basis of results for elements other than the actinides. Recently, we have calculated the atomic volumes of the $4d$ metals by the exact procedure used here for the light actinides, i.e., $4p$ semicore, two energy panels, and s , p , d , and f orbitals, and compared the results with full-potential calculations. We find that the FCD method yields atomic volumes for the metals Y, Zr, Nb, Mo, Tc, Ru, Rh, and Pd, which on the average are only 1% larger than the corresponding full-potential calculations.¹⁵ Hence, we expect the full-charge density results presented in Figs. 1 and 2 to represent an accurate estimate of the true local-density atomic volumes of the actinide metals in their α phases.

IV. CONCLUSION

Based on the above considerations, it appears that the full charge-density results, shown in Fig. 1, represent a close approximation to the true local-density values, at least for the

the earlier actinides, Fr–U, where spin-orbit coupling does not affect the volumes in a significant way. Furthermore, the fact that the calculated volume is a decreasing function of the atomic number similar to the fcc results means that in the LDA the crystal structures are not responsible for the increasing difference between theory and experiment as one approaches Pu. Based on earlier LMTO-ASA calculations it seems that spin-orbit coupling may explain half of the discrepancy in Pu and that therefore the remainder may be attributed to correlation effects not included in the local-density approximation. However, such a conclusion must await calculations including not only the correct crystal structures for Np and Pu but also spin-orbit coupling.

ACKNOWLEDGMENTS

This work was supported in part by Grant No. ERB-CIPA-CT-92-2096 of the Commission of the European Communities and Research Project Nos. OTKA 2950 and 016740 of the Hungarian National Scientific Research Foundation. Center for Atomic-scale Materials Physics is sponsored by the Danish National Research Foundation.

APPENDIX

The step function $\Theta_R(\mathbf{r}_R)$ in Eq. (8) may be expanded in terms of real harmonics, i.e.,

$$\Theta_R(\mathbf{r}_R) = \sum_L \Theta_{RL}(r) Y_L(\hat{\mathbf{r}}),$$

where the partial components $\Theta_{RL}(r)$ are

$$\Theta_{RL}(r) = [\pi(2l+1)]^{1/2} \frac{1}{2^l} \sum_{k \geq l/2}^l (-1)^{k+l} \begin{pmatrix} l \\ k \end{pmatrix} \begin{pmatrix} 2k \\ l \end{pmatrix} \times \frac{1 - \left(\frac{r^2 + R^2 - S_R^2}{2rR} \right)^{2k-l+1}}{2k-l+1} D_{0m}^l(\hat{\mathbf{R}})$$

and $D_{0m}^l(\hat{\mathbf{R}})$ are the matrix elements of finite rotations defined, for example, in Ref. 29.

The energy moments in Eq. (14) are given by

$$m_{R'L'R''L''}^{pq} = \sum_{j,occ.} (E_j - E_{vR'L'})^p b_{R'L'}^{j*} (E_j - E_{vR''L''})^q b_{R''L''}^j,$$

where b_{RL}^j denote the eigenvectors and E_j the one-electron energies obtained from the band calculation.

The quantities $G_{R'L'R''L''}^{pqL}(r)$ in Eq. (14) are defined as

$$G_{R'L'R''L''}^{00L}(r) = \delta_{R'0} \delta_{R''0} C_{L'L''}^L \varphi_{0L''}(r) \varphi_{0L'}(r) + \delta_{R'0} \varphi_{0L'}(r) \times \sum_{L'''} C_{L'L'''}^L F_{R''L''}^{L'''}(r) + \delta_{R''0} \times \sum_{L'''} C_{L''L'''}^L F_{R'L'}^{L'''}(r) \varphi_{0L''}(r) + \sum_{L'''} F_{R'L'}^{L'''}(r) \sum_{L''''} C_{L''L''''}^L F_{R''L''}^{L''''}(r),$$

$$G_{R'L'R''L''}^{01L}(r) = \delta_{R'0} \delta_{R''0} C_{L'L''}^L \varphi_{0L'}(r) \dot{\varphi}_{0L''}(r) + \delta_{R''0}$$

Here

$$\times \sum_{L'''} C_{L''L'''}^L F_{R'L'}^{L'''}(r) \dot{\varphi}_{0L'''}(r),$$

$$G_{R'L'R''L''}^{10L}(r) = G_{R''L''R'L'}^{01L}(r),$$

and

$$G_{R'L'R''L''}^{11L}(r) = \delta_{R'0} \delta_{R''0} C_{L'L''}^L \dot{\varphi}_{0L'}(r) \dot{\varphi}_{0L''}(r).$$

$$F_{R'L'}^L(r) = \sum_{L''L'''} C_{L''L'''}^L f_{R'L'L''}(r) \Theta_{R'L'''}(r),$$

with $f_{R'L'L''}(r)$ defined from Eq. (13). In these expressions R' and R'' run over neighbors with overlapping ASA spheres.

-
- ¹H.L. Skriver, O.K. Andersen, and B. Johansson, Phys. Rev. Lett. **41**, 42 (1978).
²M.S.S. Brooks, B. Johansson, and H.L. Skriver, in *Handbook on the Physics and Chemistry of the Actinides*, edited by A.J. Freeman and G.H. Lander (North-Holland, Amsterdam, 1984), Vol. 1, p. 153.
³B. Johansson, R. Ahuja, O. Eriksson, and J.M. Wills, Phys. Rev. Lett. (to be published).
⁴M.S.S. Brooks, J. Phys. F **13**, 103 (1983).
⁵P. Söderlind, L. Nordström, L. Yongming, and B. Johansson, Phys. Rev. B **42**, 4544 (1990).
⁶J.M. Wills and O. Eriksson, Phys. Rev. B **45**, 13 879 (1992).
⁷J. van Ek, P.A. Sterne, and A. Gonis, Phys. Rev. B **48**, 16 280, (1993).
⁸O. Eriksson, J.M. Wills, P. Söderlind, Joost Melsen, R. Ahuja, A.M. Boring, and B. Johansson, J. Alloys Comp. **213/214**, 268 (1994).
⁹P. Söderlind, O. Eriksson, B. Johansson, and J.M. Wills, Phys. Rev. B **50**, 7291 (1994).
¹⁰P. Söderlind, J.M. Wills, B. Johansson, and O. Eriksson, Phys. Rev. B (to be published).
¹¹L. Vitos, J. Kollár, and H.L. Skriver, Phys. Rev. B **49**, 16 694 (1994).
¹²J. Kollár, L. Vitos, and H. L. Skriver, Phys. Rev. B **49**, 11 288 (1994).
¹³L. Vitos, J. Kollár, and H. L. Skriver (unpublished).
¹⁴D.A. Young, *Phase Diagrams of the Elements* (University of California Press, Berkeley, 1991).
¹⁵V. Ozolins and M. Körling, Phys. Rev. B **48**, 18 304 (1993).
¹⁶O.K. Andersen, Phys. Rev. B **12**, 3060 (1975).
¹⁷H.L. Skriver, *The LMTO Method* (Springer-Verlag, Berlin, 1984).
¹⁸O.K. Andersen, Z. Pawlowska, and O. Jepsen, Phys. Rev. B **34**, 5253 (1986).
¹⁹O.K. Andersen, A.V. Postnikov, and S.Yu. Savrasov, in *Applications of Multiple Scattering Theory in Materials Science*, edited by W.H. Butler, P.H. Dederichs, A. Gonis, and R.L. Weaver (Materials Research Society, Pittsburgh, PA, 1992), pp. 37–70.
²⁰O.K. Andersen and R.G. Woolley, Mol. Phys. **26**, 905 (1973).
²¹L. Vitos, J. Kollár, and H. L. Skriver, in *Stability of Materials*, Vol. 355 of *NATO ASI Series E: Applied Sciences*, edited by A. Gonis, P.E.A. Turchi, and J. Kudrnovsky (Kluwer Academic Publishers, The Netherlands, 1995), pp. 393–399.
²²A. Gonis, E.C. Sowa, and P.A. Sterne, Phys. Rev. Lett. **66**, 2207 (1991).
²³L. Vitos and J. Kollár, Phys. Rev. B **51**, 4074 (1995).
²⁴J. Perdew and A. Zunger, Phys. Rev. B **23**, 5048 (1981).
²⁵D.M. Ceperley and B.J. Alder, Phys. Rev. Lett. **45**, 566 (1980).
²⁶O.K. Andersen, O. Jepsen, and D. Glözel, in *Highlights of Condensed-Matter Theory*, edited by F. Bassani, F. Fumi, and M.P. Tosi (North-Holland, New York, 1985).
²⁷W.R. Lambrecht and O.K. Andersen, Phys. Rev. B **34**, 2439 (1986).
²⁸D.G. Pettifor, Commun. Phys. **1**, 141 (1976).
²⁹A.R. Edmonds, *Angular Momentum in Quantum Mechanics*, edited by Eugene Wigner and Robert Hofstadter (Princeton University Press, Princeton, 1957).